

Ignition Study at Small-Scale Solid Rocket Motor

Olivier Orlandi*, Fabien Fourmeaux**, Joël Dupays #

* ArianeGroup

Les cinq Chemins, 33185 Le Haillan, France, olivier.orlandi@ariane.group

** ArianeGroup

Centre de Recherches du Bouchet, rue Lavoisier, 91710 Vert-le-Petit, France

ONERA

Centre de Palaiseau, Chemin de la Hunière, 91710 Palaiseau

Abstract

This paper presents the approach adopted at ArianeGroup for the study of ignition in Solid Rocket Motors. A focus is made on the necessary stages to perform a calculation of the firing of a small-scale SRM. The first step consists in characterising the thermal properties of the propellant. The second step addresses the determination of the ignition time for a small sample of propellant subjected to a given flux. A first validation of the numerical model is obtained with the simulation of such tests. A dedicated test was designed to measure the flame spreading over the propellant surface sample. As for the ignition time, the model successfully predicts the measured velocity. Finally, it is applied to the simulation of the ballistics of a small-scale firing. Understanding elements were obtained on the physics involved in the ignition process. This last stage validates the overall approach and allows its use to the simulation of the ignition of full-scale SRM.

Keywords: Ignition modelling, Ignition time, Ignition model, Flame spreading, SRM

Nomenclature

A_p	Pre-exponential factor
E_g	Activation energy in the gas phase
E_p	Activation energy in the solid phase
C_p	Heat capacity
\dot{m}_p	Instantaneous Propellant mass flow rate
Q_s	Heat release by surface reactions
R	Perfect gas constant
T	Temperature
α	Thermal diffusivity of the propellant
λ	Thermal conductivity
Φ_{conv}	Convective flux
Φ_{flam}	Flame flux
Φ_{rad}	Radiative flux
ρ_p	Propellant volumetric mass
\cdot_p	Relative to propellant

Acronyms

AP	Ammonium Perchlorate
HTPB	Hydroxyl-Terminated-Poly-Butadiene
MF	« Mesure de Flux » (Flux measure)
SRM	Solid Rocket Motor

1. Introduction

Transient phases during Solid Rocket Motors (SRM) operating have to be studied with a specific care and modelled with accuracy. Regarding these events, ignition is a critical phase: pressure oscillations can induce strong mechanical stresses into the engine structure [1]. ArianeGroup has developed a dedicated approach based on experimental

characterizations and numerical simulations to better understand and master physical phenomena involved in the ignition of SRMs. This paper presents the different steps required to simulate the ignition of a small scale study motor (hereafter called “MF”). The considered propellant is a common non-aluminised composite propellant. The oxidizer loading is composed of ammonium perchlorate (AP) and the binder is based on a standard HTPB rubber. The aim of the study is to validate the numerical modelling of the ignition phase and how to process data in the scaling-up from elementary characterization of the propellant to the simulation of the experimental small-scale motor MF.

Ignition is a transient phenomenon [2] that can roughly be divided into two parts. Firstly a thermal flux heats up the propellant surface. Then the heat diffuses inside the material. It is generally considered that the propellant remains as “inert” and no chemical reaction can be clearly identified. When its surface temperature is sufficiently high, the ignition can take place. It is characterized by the occurrence of chemical reactions at the propellant surface and production of gases that will react into combustion products. That transient step finally results in the stationary combustion of the propellant. A detailed description of the phenomenon is proposed in [3] by Gallier *et al.* where the ignition process is simulated at a mesoscopic scale representing the loading components of the propellant.

In order to correctly describe these physical phenomena, ArianeGroup develops a specific approach to consolidate and validate the numerical tools which are used in the simulation of the ignition of solid rocket motors. For this purpose, small scale motors are fired and analysed. In order to acquire a correct restitution of the ballistics, a first step is dedicated in the characterization of the thermal properties of the propellant. Density, thermal conductivity and heat capacity are assessed at room temperature and ambient pressure. This stage is essential for any further modelling subsequent of the thermal behaviour of the solid propellant. The second step regards the determination of the ignition time for a small sample of propellant subjected to a specified heat flux. Numerical models used for the ignition are then tested on these experimental data. Based on the resolution of the heat transfer equations into the solid materials with a specific treatment on the surface where the energy balance is assessed with more or less accuracy, it is possible to reproduce the surface temperature evolution. These specific models are of prime importance to correctly describe the physics of the ignition. Such models are implemented into the CFD code developed by Onera [4] and preferentially used by ArianeGroup for the ignition studies. However, available models require the robust determination of a set of parameters. A third step then consists in the simulation of the flame spreading at the surface of the propellant. A dedicated experimental set up was designed to access this information and the closure of the model is ensured by numerically obtaining the measured flame spreading velocity. The last stage considers the application of the identified model to the ignition of a small-scale study motor. It consists in a 7kg cylindrical grain with a central bore. The ignitor is a small micro-rocket with 6 blowholes. Preliminary calculations aim at defining the mass flow rate and the temperature of gases of this ignitor. A 3-dimensional numerical simulation is then performed to study the ignition of the grain and provide a better understanding of the physical phenomena.

2. Ignition modelling

All the numerical simulations presented in this study are performed with the in-house Onera code. Compressible Navier-Stokes equations with two equation turbulence model are solved using a finite-volume technique on unstructured mesh. A RAMS approach for the gas and condensed phase is considered and calculations are performed at second order accuracy in space (Roe scheme) and first order accuracy in time with an implicit scheme. Dedicated models have then been implemented to describe the non-steady ignition of the propellant. Two more or less complex models have been developed and integrated into the numerical tool by Onera. They will be respectively referred as model A and model B. Some details can be found in [5]. Both considered the resolution of the heat conduction into the inert materials.

2.1 Thermal consideration

The standard equation of heat diffusion is associated to the energy equation into the propellant. This material is modelled as homogeneous, that means that all the structure of the composition propellant (i.e. AP loads) is not considered. For model A, the thermal equation can be written as, in a one-dimensional formalism:

$$\frac{\partial T}{\partial t} = \alpha \frac{\partial^2 T}{\partial y^2}$$

where α is the thermal diffusivity of the propellant.

Model A describes the ignition phase in an unsteady way, but the solution of the thermal transfer equation does not allow to reach the steady state since it is not stabilized by the convection term related to the propellant combustion

rate. This limitation is removed in model B which solves the complete equation that translates the unsteady heating of the propellant by conduction and its surface decomposition at combustion rate V_c :

$$\frac{\partial T}{\partial t} + V_c \frac{\partial T}{\partial y} = \alpha \frac{\partial^2 T}{\partial y^2}$$

At the propellant surface, for both models, the conductive thermal flux of the material is balanced by fluxes from the gas phase (convective and radiative fluxes) and the heat released by the propellant degradation at the surface:

$$\lambda_p \frac{\partial T}{\partial x} = (1 - \beta)\Phi_{flam} + \beta(\Phi_{conv} + \Phi_{rad}) + \dot{m}_p Q_s$$

where β is a parameter that can switch from the non-stationary state during the ignition to the stationary combustion state.

2.2 Flame structure of the ignition models

The model ‘‘A’’ is a very simple model to describe the ignition process. It is based on the heat diffusion into the material and the propellant mass flux rate due to the external heat flux is modelled by an Arrhenius law:

$$\dot{m}_p = \rho_p A_p e^{\left(\frac{-E_p}{RT_s}\right)}$$

This indicates that, in this model, no flux from the propellant flame is considered and β is taken equal to 1. The ignition occurs by comparing the surface temperature in the reactive case (with the above definition of \dot{m}_p) and in the inert case. When the difference between the two surface temperatures evolution exceeds a given value (let’s say 5%), it is assumed that the propellant locally ignites. The complete combustion is taken after an addition time to reach the stationary combustion state.

The model ‘‘B’’ is more representative of the complexity of the propellant flame. It is moreover assumed that the propellant is a homogeneous material. This approach cannot describe the small flame structure that takes place at the propellant surface. Neither premixed flame at the AP loads nor diffusion flame between HTPB degradation and AP combustion products gases are considered. Whatever, a general evolution of the temperature is assumed from the propellant surface temperature to the combustion gas temperature. Without entering into details, an additional equation is added to describe the overall reactions in the gas phase. A premixed flame is considered through a second Arrhenius law and its associated E_g activation energy in the gas phase.

To summarise, the ignition models require the determination of three parameters (A_p , E_p and Q_s) for the model ‘‘A’’ and four parameters (the three previous ones plus E_g) for the model ‘‘B’’. An important task will be devoted to the determination of these parameters so that the models can describe the ignition physics of the propellant. Experimental data are then mandatory to fit the observed ‘‘ignition times’’ with the selected model.

2.3 Radiative and convective fluxes

The global flux received by the propellant surface can be split into two major contributions. The major part is provided by the convection at the propellant surface. As a description of the boundary layer could be exhaustive in term of number of cells, a dedicated boundary layer condition has been introduced into the numerical code to correctly estimate the exchange coefficient ‘ h ’ thanks to a dedicated boundary model.

The radiation solver used in this study is based on a discrete ordinate method. It was specifically developed by Onera to solve radiative problems applied to solid propulsion [6].

3. Propellant characterisation

For the purposes of illustration and simplification, this study considers a AP/HTPB composite propellant. No aluminium is added to the formulation so that two-phase effects are then not considered. If the propellant would have contained additional metallic powders (aluminium for instance), the determination of the radiative flux should have taken into account the presence of alumina smoke in the combustion products. Only gaseous molecules are at the

origin of the radiative flux and its value is so low compared to the convective flux that it is finally considered as non-significant.

The considered propellant is then composed of AP for the main loading with a HTPB based binder.

3.1 Thermal properties

The evaluation of the thermal diffusivity and effusivity requires the knowledge of the propellant volumetric mass, thermal conductivity and thermal conductivity. The next table summarizes the values of the thermal properties used in this study:

Table 1 : thermal properties of the tested propellant

	Value
density (Kg/m^3)	~ 1700
Heat Capacity (J/Kg/K)	~ 1100
Thermal conductivity (W/m/K)	~ 0.4

3.2 Experimental Ignition time / Flux test bench

The ignition times are crucial data to validate the ignition models. The BALBEC (Banc d'Allumage Balistique et Combustion) test bench developed by ArianeGroup allows to obtain ignition times depending on various radiative fluxes provided by a CO_2 laser. Before the test, the power provided by the laser beam is tested and calibrated on a specific propellant. The following figure provides an illustration of the bench. The ignition of the propellant sample is ensured by the laser beam for which a specific power was selected in the range of those that are encountered in a SRM (roughly around 1MW/m^2). A laser diode provides an electric tension according the light detected in the vessel. The ignition time is then determined when the light emissivity starts to increase significantly. Considering the flux received by the sample, it is estimated thanks to the power emitted divided by the total surface impacted by the laser beam. The surface is measured before each firing on a PMMA sample.

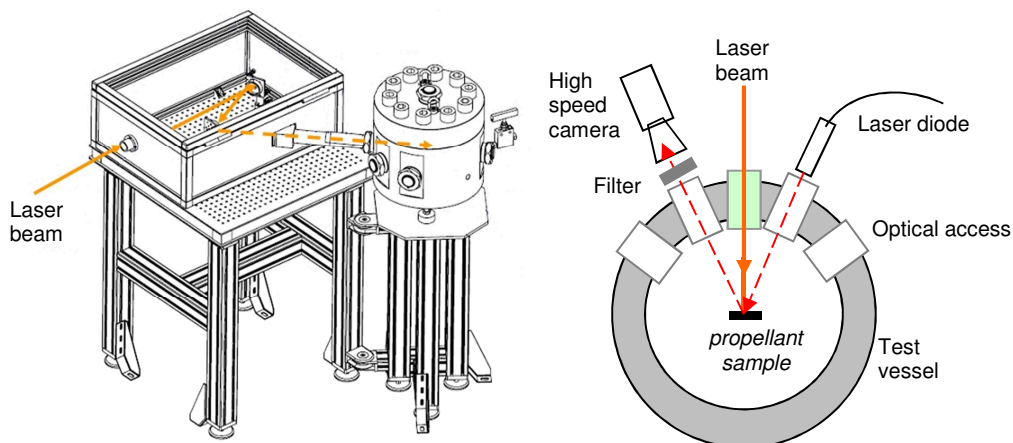


Figure 1 : Ignition test bench BALBEC
(general view and location of instrumentation for flame propagation measurement)

Thanks to the BALBEC test bench, the ignition times versus three different heat fluxes were measured for the AP/HTPB composite propellant. The results are reported to the next figure. In a log-log representation, the experimental data are located along a straight line whose slope of -2 is characteristic of the evolution of the ignition times with the flux.

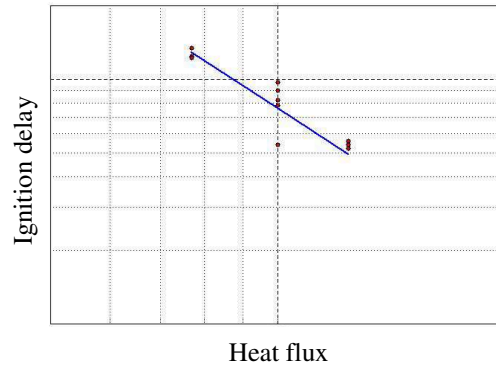


Figure 2 : Ignition time vs. total heat flux

4. Parameters fitting

This phase is of prime importance to define the ignition model. It is based on the exploitation of experimental data such as ignition time vs. heat flux. These data are completed by the evaluation of the flame spreading velocity over the propellant surface. The optimized set of parameters has to correctly estimate the experimental results.

4.1 Ignition time test exploitation

From the exploitation of the ignition time, it is possible to access the knowledge of the parameters required by the different models. It has to be noted, that the parameters which are obtained for a model A cannot be applied directly to a model B and a new evaluation phase will have to be launched. A common way to find the values of parameters lays on a least square minimization optimization. To achieve this goal, the two models were introduced in an in-house optimization tool. This was applied to the present study, but depending on the bounds for the solutions (initial and conditions) imposed in the procedure, several set of parameters can be found. Unfortunately, we reach the limit of such an approach. For example, the value of Q_s may be positive for a surface reaction releasing energy or negative for an endothermic process. An illustrative case is proposed considering the model B. Several sets of parameters have been identified and corresponding results are reported in the following table. The ignition times are non-dimensionalized by the time measured at the intermediate flux. Both sets of parameters provide good approximation even if the set #4 seems to render the best ignition times for the lowest flux.

Table 2 : normalized experimental ignition times and application of model B for two different sets of parameters

Flux	Experimental	set of parameters #3	set of parameters #4
lowest	1.89	1.51	1.67
Medium	1.00	0.96	1.04
highest	0.66	0.67	0.69

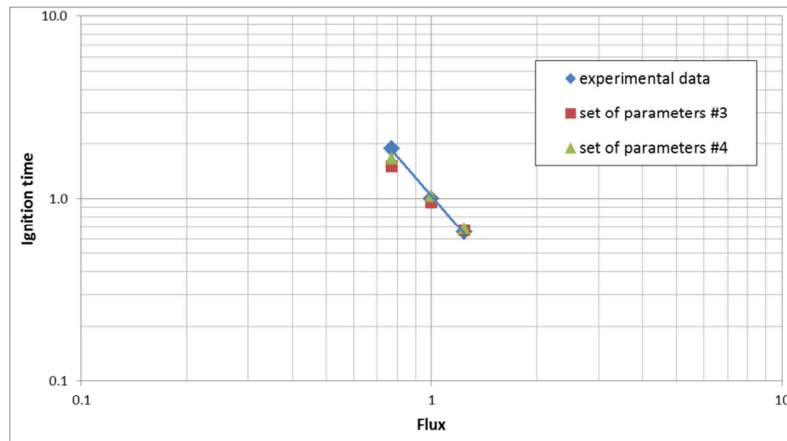


Figure 3 : Non-dimensioned ignition time vs. total non-dimensioned heat flux for the experimental data and application of model B

4.2 Flame spreading exploitation

For this experimental test, the test bench BALBEC is used to ignite and record the expansion of the flame over the propellant surface. The Figure 4 presents a sketch of different views of the ignited propellant surface. A square sample is ignited at its centre by a laser beam. In a first step, the laser is not turned off as soon as the propellant starts to burn in order to ensure a good ignition. After 0,5s, the laser is turned off and a self-combustion occurs. One observes the propagation of the flame over the surface according a disk whose diameter increases regularly with time.

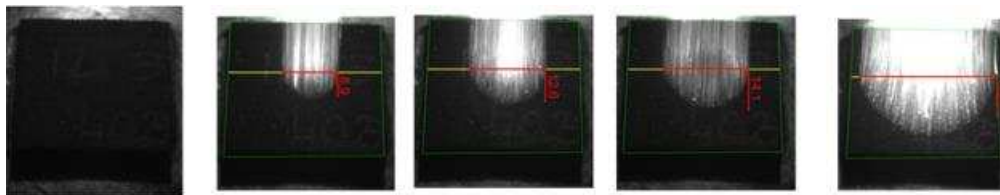


Figure 4 : Pictures of the flame spreading at different times

A numerical treatment of the movie was performed to better evaluate the spreading velocity of the flame. By analyzing each frame of the movie, it was possible to determine the diameter of the hot gases column. This information is plotted on Figure 5 and derivation of the flame position gives a value of 4.5 mm/s for the velocity.

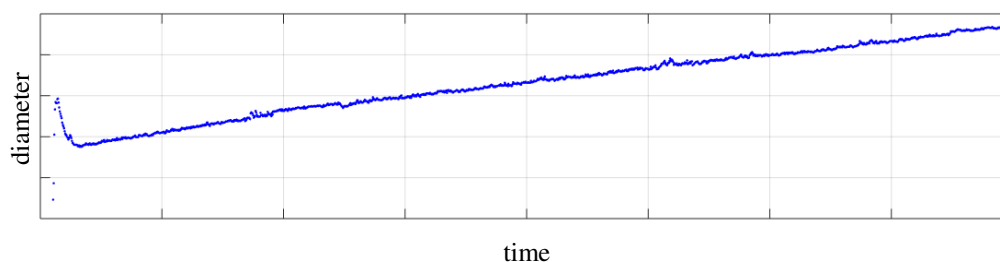


Figure 5 : Pictures of the flame spreading at different times

A restitution of the flame spreading test was performed with the Onera code. A 2D-axisymmetric regular mesh is supposed to describe the aerodynamic field composed by 5600 cells. Boundary layers are represented by ambient air conditions with a pressure of 1 bar. The last boundary layer represents the propellant surface and is divided into two parts. The first one characterized by a length of 5mm corresponds to the surface already ignited. The mass flow rate is representative of the self-combustion of the propellant for that pressure. The gas is ejected at the temperature of 2686K obtained from a thermo-equilibrium simulation (in-house code). The second part of the domain represents the surface that is about to ignite. A model "B" with the set of parameters #4 is applied. As it is supposed that the

convective flux is reduced (gas is ejected from the ignited surface in a perpendicular direction of the spreading one), the radiative solver REA [6] is activated.

The Figure 6 shows the computational domain with the location of the boundary layers. The data are as follows:

- Mass flow rate : 3 kg/m²/s
- Gas temperature of the combustion products : ~2700K
- External gas temperature : 300K
- Pressure : 1 bar

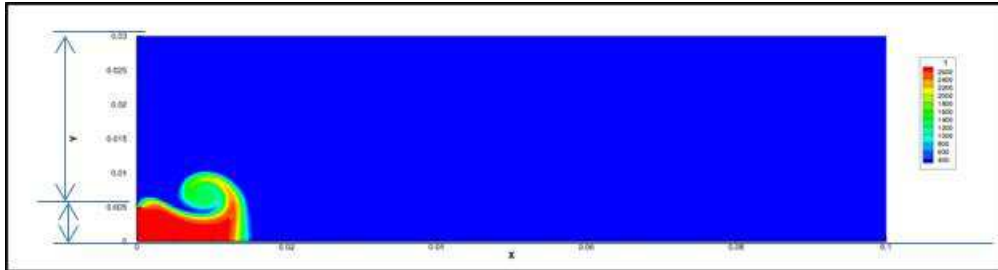


Figure 6 : Calculation domain (at 2 ms of simulation)

Radiative flux is obtained by considering the following gas species mixture: (CO/CO₂/H₂/H₂O/HCl/N₂).

The next figure shows the column of hot gases coming from the ignited surface. With time, the thickness of the burning surface increases. By deriving this thickness, it is easy to find the corresponding flame spreading velocity.

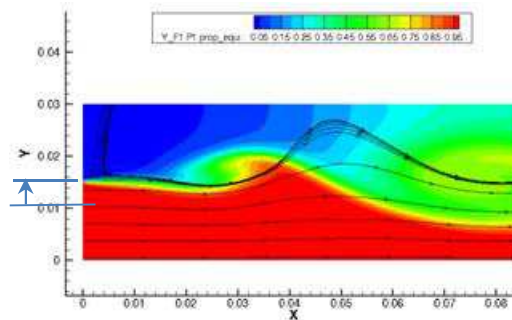


Figure 7 : Flow field after 5mm propagation of the burning (~2s of simulation)

Two experimental tests were performed and both provided very similar results and two tendencies can be observed. The first one corresponds to the time period when the laser is operating and provides an additional heat flux to the propellant. In that case, the experimental velocity is roughly 6.4 m/s. The second time period is characteristic of a self-propagating flame (laser off). The laser extinction is not taken into account in the numerical simulation. It is simply assumed that a reduced zone of the overall surface is ignited. After a quick period of time corresponding to the heating of the non-ignited part, one can observe a regular growth of the ignited surface. At 3s of simulation, the previous tendency disappears and a rapid increase is observed showing the ignition of the all propellant surface. All these stages are plotted on Figure 8 where the experimental results are added. Two tests have been performed corresponding respectively to the blue and red plots. The velocity is given by the slopes of the curves. A velocity of 3.67m/s is found for the numerical simulation to be compared to the experimental value of 4.4m/s. The similarity of the two velocities demonstrates that the model can predict the flame propagation phenomenon with a quite good accuracy

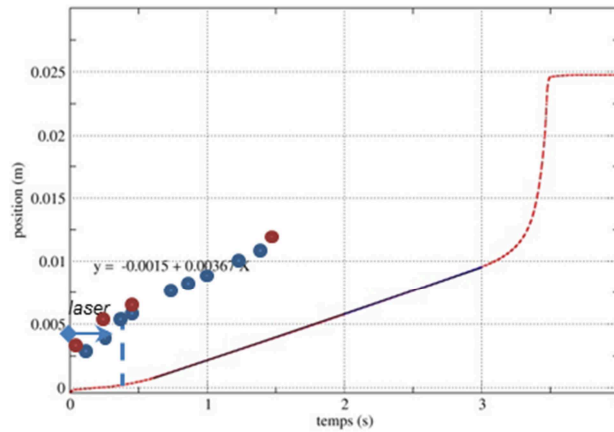


Figure 8 : Position of the limit of the ignited zone (AP/HTPB test) test are represented by blue and red plots and the exploitation of the numerical simulation by the line segment

5. Small-scale firing test

Thanks to the flame spreading test, the proposed parameter set was validated in the presence of a convective stream. The selected parameters are then able to correctly predict the ignition time under a given flux. Moreover, the proposed model can also forecast the dynamics of the flame on propellant surface. Before applying this approach to the simulation of a full scale SRM, a preliminary test is performed on a small-scale SRM. To achieve such a goal, a solid grain with central bore is fired in the MF test bomb.

5.1 MF motor

The experimental test motor “Mesure de Flux (MF)” was designed to study the ignition of a solid grain. The geometry is cylindrical with a central bore. The total length is 350mm for an outer diameter of 170mm. The overall mass of propellant (depending on the formulation) is around 7kg. Originally, the motor is equipped with 16 flux devices to access the total and radiative fluxes along the central bore as shown on Figure 9 but this possibility was not used in the present study.

The ignition of the grain is ensured by a small grain of the same formulation. The hot gases generated during the operating of the ignitor are ejected through 6 small blowholes and then form 6 plumes in the combustion chamber that will impact the inner surface of the main grain. It ignites in its turn mainly thanks to the convective fluxes. The nozzle is equipped with a diaphragm that allows the pressure to increase up to 2.4MPa before being released. As the gases provided by the ignitor are not sufficient to reach such a level, the diaphragm break-up guarantees the propellant grain was ignited. A firing was performed with the HTPB/AP grain that was previously characterized in this study.

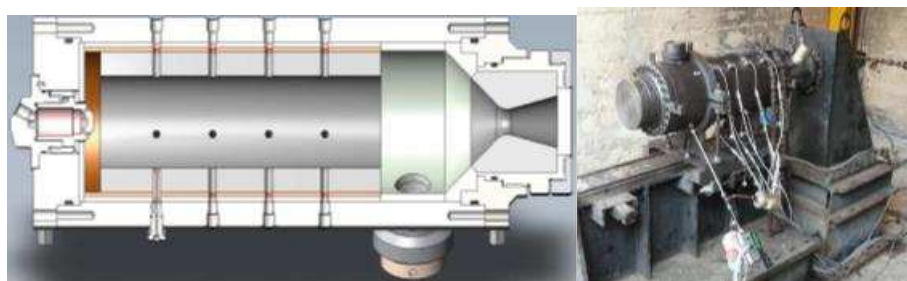


Figure 9 : MF test motor

The next figure presents the ballistics of the firing. One observes a classical pressure evolution in the combustion chamber. In a first stage, the pressure starts to slowly increase due to the injection of the gases provided by the ignitor. At 50ms, an inflection on the pressure evolution can be noticed. It indicates the beginning of the main grain

ignition. An additional mass flow rate is added to the ignitor's one. A rapid increase follows that initial pneumatic phase until the break-up of the diaphragm. Then the pressure shows a decrease occasioned by the emptying of the chamber. Finally the entire surface is ignited and the ballistic reaches the stationary pressure.

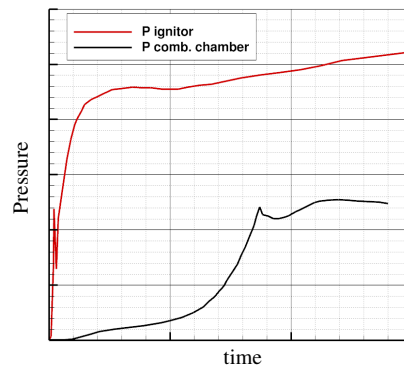


Figure 10 : Pressure history during the HTPB/AP MF firing

5.2 Exploitation of the MF firing test

The complete simulation of the firing is a complex task due to the number of physical phenomena involved. Some effects are especially important at small scale such as heat losses that may strongly influence the ballistics. In order to prepare the firing simulation, a preliminary calculation was performed to evaluate the thermal evolution of gas temperature. This step aims to provide inputs such as ignitor gas temperature with regard to the aerodynamics and a possible reduction of the communicating areas between ignitor and the combustion chamber. A 0-dimensional ballistic tool was used to simulate the evolution of the ballistics. A good agreement was obtained by considering heat losses into the ignitor that are partially compensated by a reduction of the blowholes sections. The consequence is a decrease of the gas temperature with regard to its theoretical value ($\sim 2700\text{K}$). The Figure 11 shows the evolution of the temperature of the gas in the ignitor. It increases from 2200K to 2550K when the igniting grain is completely burnt ($\sim 300\text{ms}$). An average decrease of nearly 10% on the combustion temperature is then mandatory to account for the thermal losses in the ignitor. The combustion chamber ballistic was estimated by tuning the grain surface evolution to fit the experimental results. It has no influence on the ignitor behaviour during the ignition process (i.e. for time lower than 270ms).

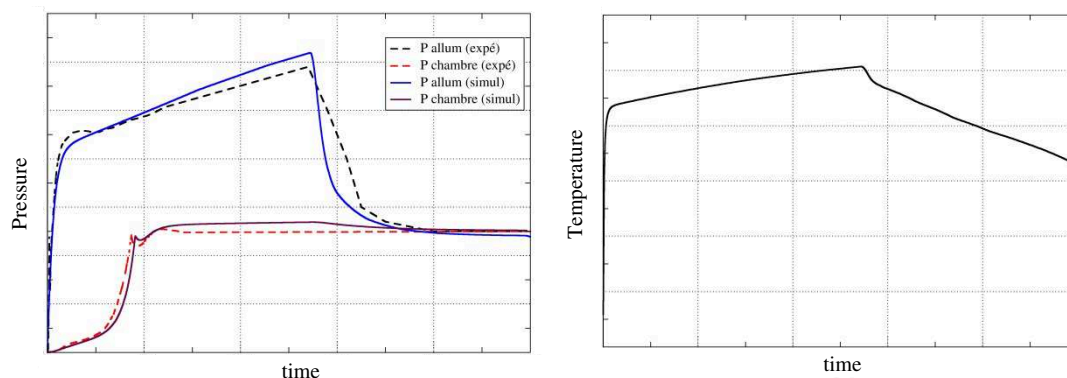


Figure 11 : 0-dimensional exploitation of the MF firing

A simulation of the ignition of the MF motor was carried out to demonstrate the capacity of the whole model to correctly reproduce the ballistics of the firing during ignition. A 3-dimensional domain is built considering the presence of the ignitor. The mesh contains 210000 cells. The model "B" with the same set of parameters as in the previous calculations was applied to represent the propellant surface transient behaviour. The Figure 12 presents the temperature flow field at the time of 0.055s . The hot gases provided by the ignitor impinge the propellant surface and are reoriented to the forward cavity. Note that at this moment, the diaphragm is still present and a vortex is created in the rear cavity. Thanks to this recirculation of the hot gases, the rear lateral surface of the grain is heated but with a certain delay compared with the central bore surface (as it will be seen on Figure 15, the convective flux is greatly reduced in this zone).

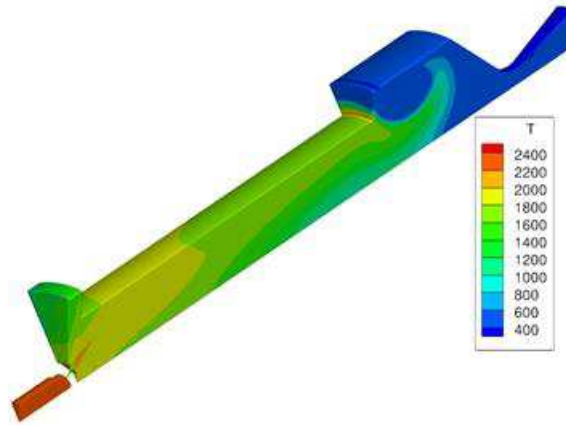


Figure 12 : Temperature flow field in the 3D simulation of the MF firing

As it can be seen on Figure 13, a good agreement is obtained between the firing pressure and the numerical results. The global evolution of the pressure is well predicted even if the experimental dynamic seems to be slower than the numerical one during the rapid increase of the pressure. The results given by applying the set #3 is also plotted in order of comparison. A more rapid ignition of the grain is obtained with this set which is coherent with the previous results on the ignition time (cf. results presented in Figure 3).

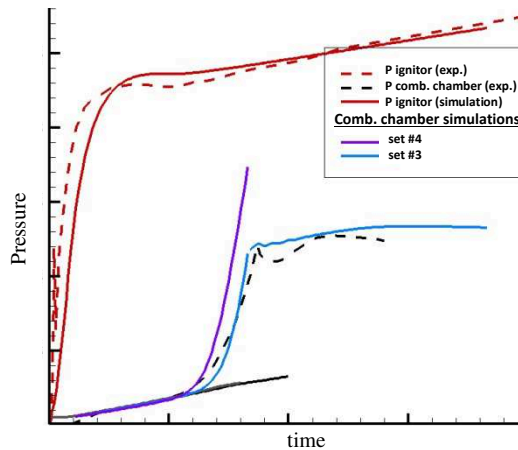


Figure 13 : Firing ballistics and its numerical restitution

A more detailed analysis of the ignition process is proposed on where the propellant surface temperature is plotted (other boundary layers are removed for clarity purpose). The ignition starts where the plume impacts the bore surface and then it propagates along the surface. The

Figure 14 illustrates this phenomenon by providing the surface temperature evolution during the heating up of the propellant. When the propellant is locally ignited, its temperature remains limited and does not go higher than 800K. The ignition spreads quickly to the whole propellant surface which explains the strong increase of the pressure until the diaphragm breaking-up.

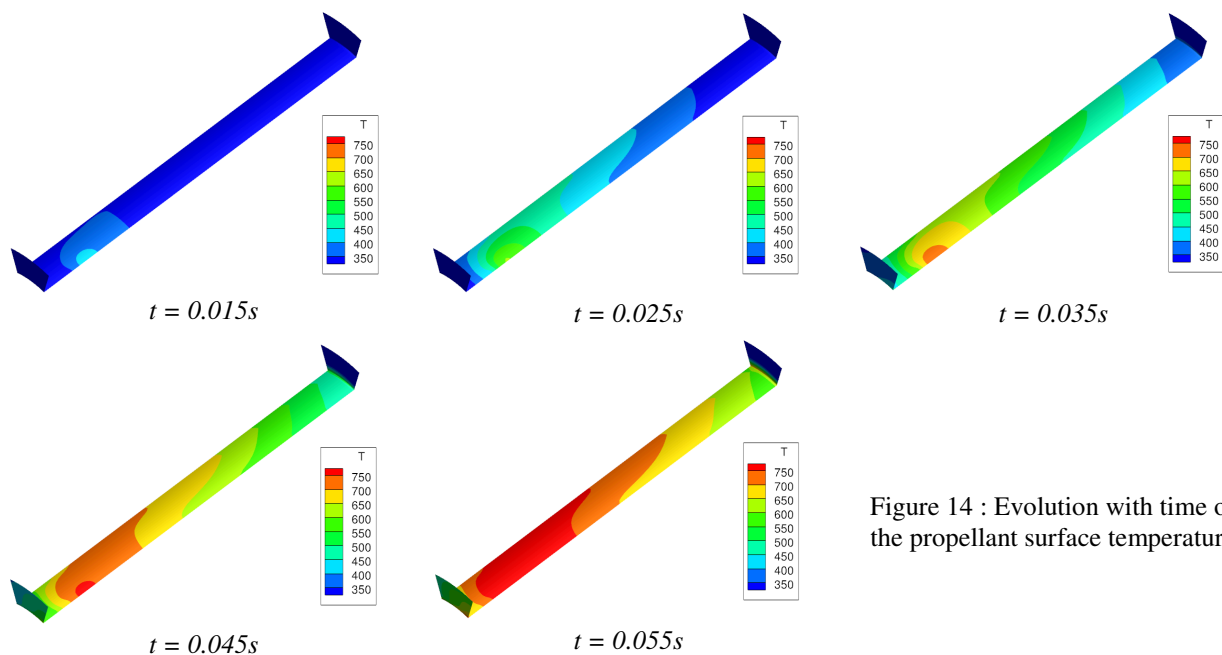


Figure 14 : Evolution with time of the propellant surface temperature

On Figure 15, the two fluxes are plotted at the time of 0.055s. One can notice the low value of the radiative flux compared to the one of the convective flux. Although the ignited propellant is limited to a zone close to the plume impact, the locations of the heat fluxes maxima are very different. The radiative flux is located immediately downstream. This corresponds to the emission of the gases provided by the propellant. Concerning the convective flux, the maximum location is at the end of the central bore. Like a wave, it begins at the impact point and moves downstream providing the major heat flux to the propellant creating temporarily a peak of flux.

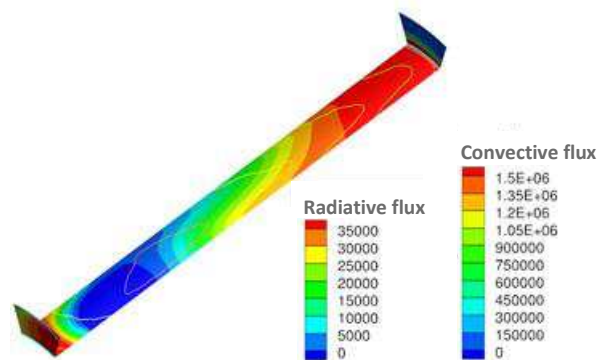


Figure 15 : Radiative (lines) and convective (contour field) fluxes at $t=0.055s$

The numerical simulation of the MF firing demonstrated the capability of the numerical chain, coupled with a dedicated ignition model (parameters determination required), to investigate the physical phenomena involved in the ignition process.

6. Conclusion

This study presents the methodology used in ArianeGroup to numerically investigate the ignition of SRM. This approach is based on both experimental and numerical tools. In a first step, a good knowledge of the propellant thermal properties is needed to access the resolution of the heat diffusion into the material. Secondly, the dependence of ignition time with respect to a given flux allows calibrating a numerical model (model A or B). The complete model is then applied to the simulation of the propellant flame spreading velocity. A good agreement between the numerical and the experimental results provides a global validation of the model. At this stage, all the physical phenomena are addressed by the modelling which is gathered in the numerical chain.

Eventually, the proposed model is applied to the calculation of the small scale Solid Rocket Motor. The firing of a AP/HTPB composition grain is successfully simulated and allows the development of such an approach for the prediction of the ignition of a scale one SRM.

Acknowledgements

The authors would like to thank the French Defence Procurement Agency (DGA) for its support. Special acknowledgments to our Onera colleagues for fruitful discussions and technical exchanges on this subject.

References

- [1] E. Cavallini, B. Favini, M. Castelli, A. Neri, « VEGA Launch Dynamic Loads due to Solid Propulsion Ignition Transient and Pressure Oscillations », 52nd Joint Propulsion Conference, July 25-27, Salt-Lake City, 2016.
- [2] G. Lengellé, A. Bizot, J. Duterque, J.-C. Amiot, « Allumage des propergols solides », La Recherche Aérospatiale, n°2, 1991, pp. 1-20.
- [3] S. Gallier, A. Ferrand, M. Plaud, « Three-dimensional simulations of ignition of composite solid propellants », Combustion and Flame, n°173, 2016, pp. 2-15
- [4] A. Refloch, B. Courbet, A. Murrone, P. Villedieu, C. Laurent, P. Gilbank, J. Troyes, L. Tessé, G. Chaineray, J.B. Dargaud, E. Quémerais, F. Vuillot « CEDRE Software », AerospaceLab Journal, Issue 2, March 2011.
- [5] A. Bizot « Ignition and unsteady combustion of AP-based composite propellants in subscale solid rocket motors », 4th Symposium on Special Topics in Chemical Propulsion (4-ISCP), Stockholm, May 27-31, 1996.
- [6] J.-M. Lamé, L. Tessé « Radiative Transfer Modeling Developed at Onera for Numerical Simulations of Reactive Flows », AerospaceLab Journal, Issue 2, March 2011.